Application Note

Noise reduction by parallel cross-correlation measurements

Zurich Instruments

Applications: Nanoelectronics, Materials Characterization, Low-Temperature Physics, Transport Measurements, DC SQUID

Products: MFLI, MFLI-DIG, MDS

Release date: May 2019

Introduction

Studying noise processes can reveal fundamental information about a physical system; for example, its temperature [1, 2, 3], the quantization of charge carriers [4], or the nature of many-body behavior [5]. Noise measurements are also critical for applications such as sensing, where the intrinsic noise of a detector defines its ultimate sensitivity. In this note, we will describe a generic method for measuring the electronic noise of a device when the spectral density of its intrinsic noise is less than that of the measurement apparatus. We implement the method using a pair of MFLI Lock-in Amplifiers, both with the Digitizer option MF-DIG.

To demonstrate the measurement, we measure the noise of a Superconducting Quantum Interference Device (SQUID) magnetometer. Typically, SQUIDs are operated by supplying a DC bias current and measuring a voltage and, as such, the limiting factor in the measurement is usually the noise floor of the voltage preamplifier. For a SQUID with gain (transfer function) $V_\Phi = 1\ \mathrm{mV}/\Phi_0$ and target sensitivity of $S = 1\ \mu\Phi_0/\sqrt{\mathrm{Hz}}$, a noise floor of $1\ \mathrm{nV}/\sqrt{\mathrm{Hz}}$ is required.

While it is possible to achieve this noise floor with some commercial amplifiers and dedicated SQUID readout electronics, most general purpose, wide bandwidth preamplifiers, such as those used in the front end of lock-in amplifiers, will only achieve a few $\mathrm{nV}/\sqrt{\mathrm{Hz}}$. Figure 1 shows the voltage noise density for the Voltage Input of an MFLI Lock-in Amplifier from Zurich Instruments. Above 1 kHz the noise floor saturates at $2.5\ \mathrm{nV}/\sqrt{\mathrm{Hz}}$ at the highest gain setting. Below 1 kHz the noise increases, reaching $7\ \mathrm{nV}/\sqrt{\mathrm{Hz}}$ at 10 Hz. Whilst these are excellent noise figures, they would be insufficient for characterizing the noise of many DC SQUIDs, particularly at low frequencies. One way of resolving signals below the noise floor of an amplifier is to make two independent measurements with two separate amplifiers and calculate the cross-correlation of their outputs [7, 8]. In an average accumulated over many such measurements, signals that are uncorrelated in the two amplifiers (e.g. amplifier noise) are attenuated, while persistent signals that are correlated are preserved.

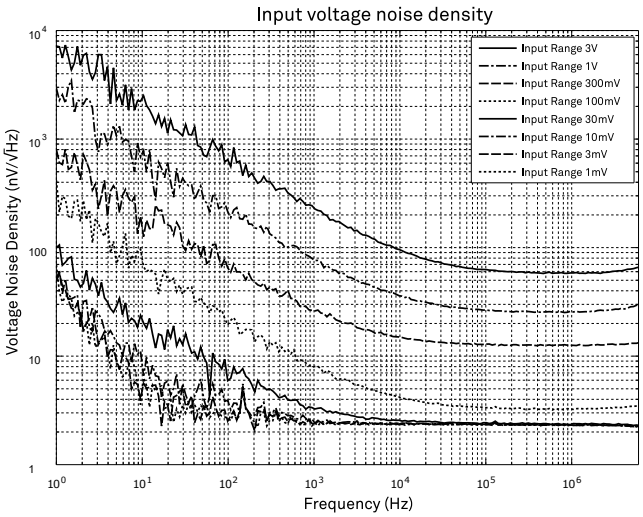

Figure 1. The voltage noise density at the Voltage Input of an MFLI Lock-in Amplifier plotted for available Input ranges [6].

To perform such a cross-correlation measurement we require two nominally identical measurement channels with the ability to sample data simultaneously in real time. Many data acquisition devices (DAQs) are not able to capture data simultaneously, and when capturing from more than one channel at a time, the samples are

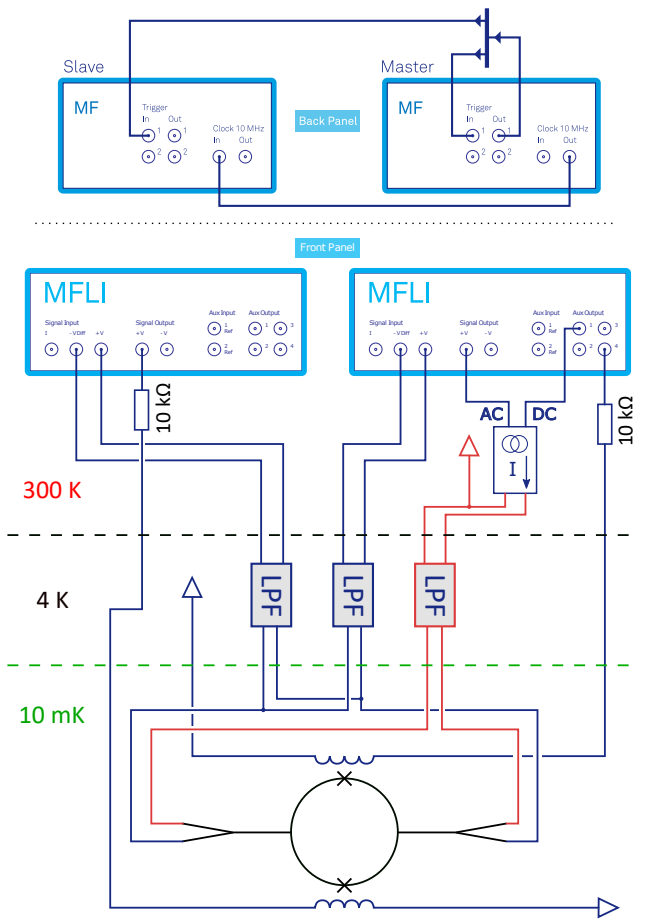

Figure 2. Top: cabling for automatic synchronization of two MFLI instruments using the multi-device synchronization (MDS) tool. Bottom: wiring schematic for noise measurements. The AC and DC voltages from the right MFLI are used to control the output of a low-noise, precision current source. There are two flux bias lines on the chip inductively coupled to the SQUID loop. We apply an AC flux using the Signal Output of the left MFLI and a DC flux using the Auxiliary Output of the right MFLI.

interleaved and the sampling rate is divided by the number of channels. DAQs that are able to sample simultaneously are typically more expensive. Using the MFLI Digitizer option we can capture up to 2.5M samples per channel at rates up to 60 MHz and with 16-bit resolution. By synchronizing the two MFLIs, we can capture this data truly simultaneously using the Zurich Instruments multi-device synchronization (MDS) provided by the LabOne® software. The MFLI has a low noise floor, which is a good starting point for the measurement. The MFLI is also a multi-functional device and we use its Auxiliary Outputs to control all other parameters of the SQUID measurement.

For this experiment, we use a four-terminal configuration to measure a DC SQUID as shown in Figure 2. The SQUID is slightly unusual in that it has graphene Josephson junctions [9, 10, 11]. The junctions have a normal state resistance of the order 50 Ω and the gain of the SQUID has a maximum around 400 $\mu V/\Phi_0$. The device is cooled below 10 mK in an Oxford Instruments Triton 400 Cryofree dilution refrigerator. The SQUID is current biased using a low-noise current source (manufactured at Lancaster University) which takes a DC voltage V_{DC} from an MFLI Auxiliary Output to set the DC current and an AC voltage V_{AC} from an MFLI Signal Output to set the AC current. In this measurement, the current supplied by the source is $(10\,\mu A/V)V_{DC} + (10\,nA/V)V_{AC}$. There are two flux bias lines on the device chip that can generate a local magnetic field in the SQUID loop. We use one to generate a DC flux by connecting it to an Auxiliary Output of an MFLI via a 10 kΩ resistor. The other flux bias line provides an AC flux by connecting it to the Signal Output of the second MFLI via a 10 kΩ resistor. With this configuration we can measure both the differential conductance and gain of the SQUID simultaneously. The voltage measurement lines connected to the SQUID are split at the coldest part of the fridge such that each channel has its own pair of wires within the cryostat. All lines are filtered with cryogenic RC filters at 4 K with a 1 MHz cut-off frequency.

We use the Digitizer option of the MFLIs to capture segments of real-time data and then calculate the discrete Fourier transform. To perform a cross-correlation, we need to capture the data from the two devices simultaneously. This is done by connecting the two MFLIs as shown in Figure 2:Top, so that each instrument uses the same clock and has a common trigger to synchronize the time stamps of both devices by MDS. We then set the Scope module on each MFLI to capture data using the common trigger. In practice, there is a small, random time offset between the two Scope traces when they initialize. We read out this time interval at the start of each acquisition and restart the Scopes if the interval falls outside a given threshold. If the initial offset is below the threshold, it will stay below the threshold for the duration of the data capture.

Cross-correlation measurements

The result of each measurement is a time series of voltages $V_1(t)$ from the first MFLI and another series $V_2(t)$ captured simultaneously by the second MFLI. Each signal has a common component $V_s(t)$, which is the signal that we wish to measure, and an independent noise component $V_{ni}(t)$:

$$V_1(t) = V_s(t) + V_{n1}(t) \quad , \qquad V_2(t) = V_s(t) + V_{n2}(t) \quad (1)$$

The cross-correlation spectrum S(f) is calculated as the dot product of the complex conjugate of the Fourier transform of one signal with the Fourier transform of the other:

$$S(f) = F[V_1(t)]^* \cdot F[V_2(t)] \quad (2)$$

The result is averaged over many repeated measurements

$$S(f)_{AVG} = \frac{\sum_{n=1}^{N} S_n(f)}{N} \quad (3)$$

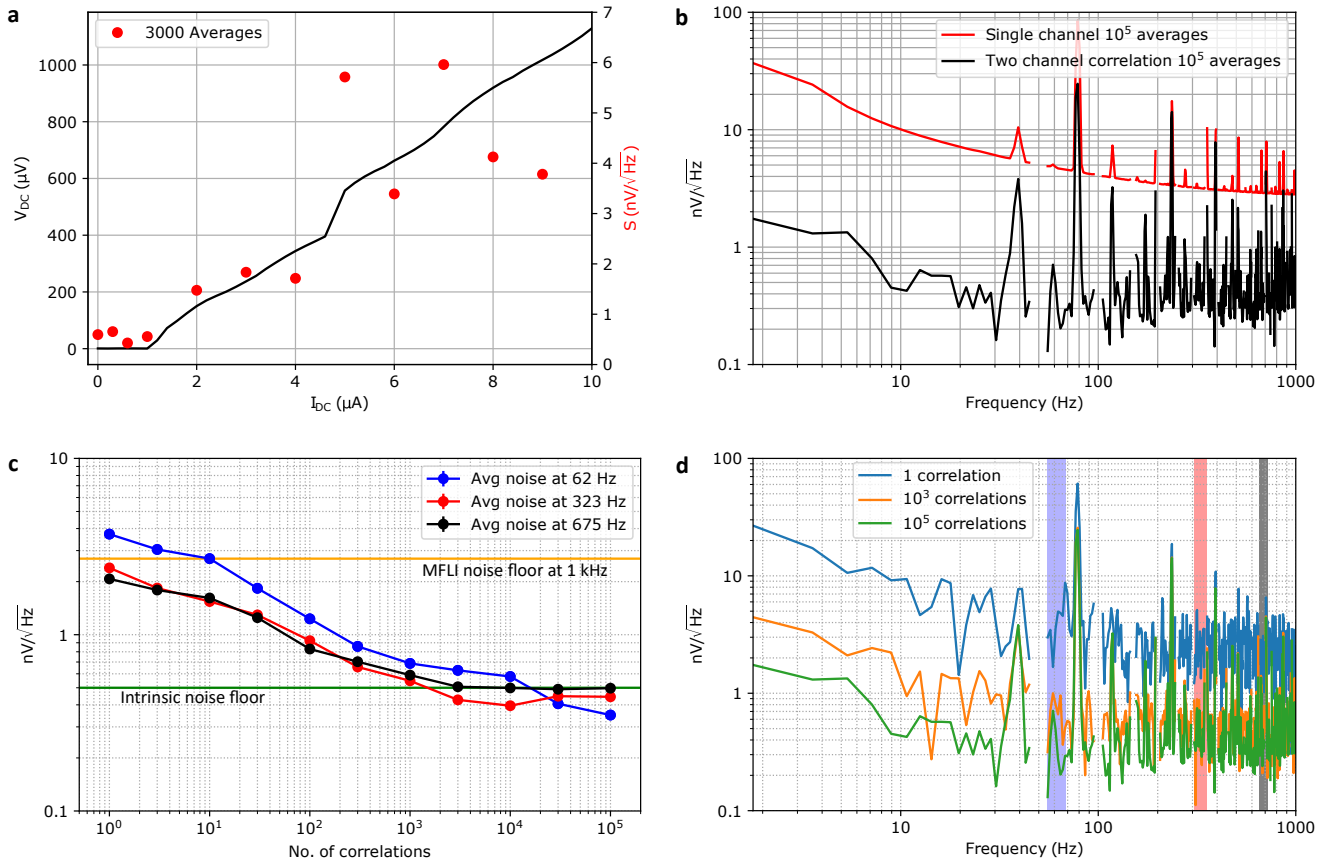

Figure 3. (a) IV characteristic (black) of the SQUID when biased at 0.5 Φ_0, minimum gain, and average noise around 62 Hz (red) taken at different points along the IV curve. (b) Noise spectrum from a single channel with 10^5 averages and noise spectrum after correlating two channels with 10^5 averages (black). (c) Correlated noise power spectral density around 62, 323 and 675 kHz as a function of the number of averages. The noise floor of the correlated measurement is around 0.5 nV/$\sqrt{\text{Hz}}$. (d) Correlated noise spectra after 1, 10^3 and 10^5 averages. The curves have been smoothed for clarity. The blue, red and black shaded areas show the regions used for panel c. Note: For all spectra, peaks at 50 Hz (mains electric frequency) and the higher harmonics have been removed for clarity.

For totally uncorrelated noise, averaging over 10^4 measurements will attenuate the noise floor by a factor of 10 (20 dB) and preserve any correlated signals.

Results and outlook

Figure 3 shows the results of characterizing our DC SQUID using the cross-correlation method. Figure 3 (b) compares a cross-correlation spectrum averaged over 10^5 measurements to the spectrum from a single MFLI with the same number of averages. Averaging a single channel gives a more precise spectrum of the single channel noise, while the average of the cross-correlation attenuates uncorrelated noise signals to reveal the spectrum of signals that are correlated between the two channels. The noise floor in the cross-correlation is much lower over the whole frequency range, reaching $\sim 0.5\,\text{nV}/\sqrt{\text{Hz}}$ above a few 10s of Hz. In Figure 3 (c) and (d) we show how the noise in the cross-correlation changes with the number of averages. Figure 3 (c) shows the reduction in the noise floor at three frequencies of interest, while Figure 3 (d) shows the full spectrum for different numbers of averages. It appears that the spectrum becomes flatter with more averages, which suggests that the uncorrelated noise has a larger 1/f component than the correlated (intrinsic) noise. This can be seen in Figure 3 (d) where at 1 kHz the noise reduces very little from 10^3 to 10^5 averages but continues to reduce around 10 Hz. Similarly, we see this in Figure 3 (c) where the noise at 62 Hz appears to reduce more than at 323 Hz and 675 Hz.

For the results shown in Figure 3 (b) to (d), the bias current was set to zero and the SQUID was fully superconducting. The intrinsic noise of the SQUID is expected to be extremely low in this state and so the results reveal the noise floor of our measurement setup. In Figure 3 (c), the noise floor is seen to saturate at $\sim 0.5\,\text{nV}/\sqrt{\text{Hz}}$ after $\approx 3 \times 10^3$ averages. From this we can conclude that there is an intrinsic noise in the device or the measurement setup of $\sim 0.5\,\text{nV}/\sqrt{\text{Hz}}$. We expect the noisiest part of the circuit to be the cryogenic filters in the current bias connections, which are 200 Ω each and will generate $0.3\,\text{nV}/\sqrt{\text{Hz}}$ of Johnson noise in total. This is a similar magnitude to the measured noise floor, but slightly too low to account for all of the correlated noise. Additional noise may come from other parts of the mea-

surement circuit, and it is also possible that the 200 Ω resistors are not fully thermalized to the 4 K stage of the fridge.

After characterizing the noise of the measurement setup, we can now use the same technique to study the noise of the SQUID in different operating conditions. Figure 3 (a) shows the IV characteristic of the SQUID when biased at a point of minimum flux sensitivity, alongside the values of the correlated noise. Note that, because we are measuring noise at relatively low frequencies, collecting a large number of averages requires long measurement times. To confirm that the SQUID does not drift from its operating point, individual signal spectra should be compared during the averaging process. In general, we have found that our graphene junction SQUIDs can be biased at a given operating point and will remain in the same condition for several days with no measurable drift. In the superconducting region, below I_C, the noise has no measurable dependence on the magnitude of the bias current and is $\sim 0.5\,\mathrm{nV}/\sqrt{\mathrm{Hz}}$. Above I_C, the noise is seen to increase with bias current. Without a correlated measurement, this behavior would be almost entirely invisible since the noise from the device only breaches the single channel noise floor above $I_{DC} \approx 5\,\mu\mathrm{A}$.

By eliminating the effect of uncorrelated noise in the voltage measurement, it becomes possible to quantify the intrinsic sensitivity of our SQUID magnetometer and allows us to study the origin of intrinsic and environmental noise affecting the SQUID. The example described above demonstrates the general utility of cross-correlation measurements when studying signals that are normally hidden below the noise floor. In this case, the noise floor of the MFLI's Input amplifier can be attenuated by using two MFLIs in parallel.

Acknowledgments

The authors of this note, Michael Thompson (m.thompson@lancaster.ac.uk), Jonathan Prance and Richard Haley (Department of Physics, Lancaster University, UK) acknowledge funding for this project from the European Union's Horizon 2020 research and innovation programme under grant agreements No 785219 and No 824109. They would also like to thank Anthony Matthews and Harriet van der Vliet (Oxford Instruments NanoScience) for helpful discussions.

References

[1] D. Rothfuß, A. Reiser, A. Fleischmann, and C. Enss. Noise thermometry at ultra-low temperatures. Philos. Trans. Royal Soc. A, (374), 2016.

[2] Z. Iftikhar, A. Anthore, S. Jezouin, F. D. Parmentier, Y. Jin, A. Cavanna, A. Ouerghi, U. Gennser, and F. Pierre. Primary thermometry triad at 6 mk in mesoscopic circuits. Nature Communications, 7:12908, September 2016.

[3] A. Shibahara, O. Hahtela, J. Engert, H. van der Vliet, L. V. Levitin, A. Casey, C. P. Lusher, J. Saunders, D. Drung, and Th. Schurig. Primary current-sensing noise thermometry in the millikelvin regime. Philosophical Transactions of the Royal Society of London A: Mathematical, Physical and Engineering Sciences, 374(2064), 2016.

[4] M. Dolev, M. Heiblum, V. Umansky, Ady Stern, and D. Mahalu. Observation of a quarter of an electron charge at the $\nu = 5/2$ quantum hall state. Nature, 452(7189):829–834, April 2008.

[5] Jesse Crossno, Jing K. Shi, Ke Wang, Xiaomeng Liu, Achim Harzheim, Andrew Lucas, Subir Sachdev, Philip Kim, Takashi Taniguchi, Kenji Watanabe, Thomas A. Ohki, and Kin Chung Fong. Observation of the dirac fluid and the breakdown of the wiedemann-franz law in graphene. Science, 351(6277):1058–1061, 2016.

[6] Zurich Instruments. MFLI User Manual, 2017.

[7] T. Chen and A. van der Ziel. Hanbury brown-twiss type circuit for measuring small noise signals. Proceedings of the IEEE, 53(4):395–395, April 1965.

[8] S. S. Wolff. On the brown-twiss circuit. Proceedings of the IEEE, 53(8):1140–1141, Aug 1965.

[9] Caglar Girit, V. Bouchiat, O. Naaman, Y. Zhang, M. F. Crommie, A. Zettl, and I. Siddiqi. Tunable graphene dc superconducting quantum interference device. Nano Letters, 9(1):198–199, 2009. PMID: 19090696.

[10] G. Nanda, J. L. Aguilera-Servin, P. Rakyta, A. Kormányos, R. Kleiner, D. Koelle, K. Watanabe, T. Taniguchi, L. M. K. Vandersypen, and S. Goswami. Current-phase relation of ballistic graphene josephson junctions. Nano Letters, 0(0), 2017. PMID: 28474892.

[11] M. D. Thompson, M. Ben Shalom, A. K. Geim, A. J. Matthews, J. White, Z. Melhem, Yu. A. Pashkin, R. P. Haley, and J. R. Prance. Graphene-based tunable squids. Applied Physics Letters, 110(16):162602, 2017.